

NUMERICAL EXPERIMENTS WITH BERGMAN KERNEL FUNCTIONS IN 2 AND 3 DIMENSIONAL CASES

S. BOCK, M. I. FALCÃO, K. GÜRLEBECK AND H. MALONEK

ABSTRACT. In this paper we revisit the so-called Bergman kernel method - BKM - for solving conformal mapping problems and propose a generalized BKM-approach to extend the theory to 3-dimensional mapping problems. A special software package for quaternions was developed for the numerical experiments.

1. INTRODUCTION

The construction of reproducing kernel functions is not restricted to real 2-dimension. Indeed, the two complex variable case has been already considered by Bergman himself (c.f.[1]). Moreover, results concerning (and restricted to) the construction of Bergman kernel functions in closed form for special domains in the framework of hypercomplex function theory (which not supposes the consideration of spaces corresponding to *even* real dimensions) can be found in [4, 5, 16].

They suggest that BKM can also be extended to mapping problems in higher dimensions, particularly 3-dimensional cases. We illustrate such a generalized BKM-approach by presenting numerical examples obtained by the use of specially developed software packages for quaternions.

2. THE COMPLEX CASE REVISITED

Let Ω be a bounded simply-connected domain with boundary $\partial\Omega$ in the complex z -plane ($z = x+iy$), and let $L^2(\Omega)$ denote the Hilbert space of all square integrable functions which are analytic in Ω . Consider the inner product in $L^2(\Omega)$

$$\langle g_1(z), g_2(z) \rangle = \iint_{\Omega} g_1(z) \overline{g_2(z)} dx dy,$$

assume w.l.o.g. that $0 \in \Omega$ and let $K(\cdot, 0)$ be the Bergman kernel function of Ω with respect to 0. Then, the kernel function $K(\cdot, 0)$ is uniquely characterized by the *reproducing property*

$$\langle g, K(\cdot, 0) \rangle = g(0), \quad \forall g \in L^2(\Omega).$$

Date: 2003.

1991 Mathematics Subject Classification. AMS.

Key words and phrases. Numerical conformal mapping, Bergman kernel, quaternions.

The kernel function $K(\cdot, 0)$ was introduced by Bergman in 1921. He spent most of his life developing properties and applications of his kernel function, in particular, to conformal mapping.

One of the most important aspects of conformal mappings is the persistence of solutions of Laplace's equation. This property is very useful in physical problems involving Laplace's equation, such as electrostatics, heat flow, fluid mechanics, etc. In fact, once the equation has been solved on a particular domain, the solution is immediately known on all domains which can be mapped onto the original via a one-to-one analytic function.

There are several methods for solving conformal mapping problems. In contrast to most conformal mapping techniques, the approximation of the solution obtained by using the Bergman Kernel method is an analytic function.

2.1. The Bergman Kernel Method.

The Bergman Kernel Method - BKM is a method for approximating the conformal map

$$f : \Omega \rightarrow D := \{w : |w| < 1\}, \text{ such that } f(0) = 0 \text{ and } f'(0) > 0.$$

The method is based on the *reproducing property* (2) of the kernel function and on the well known relation of $K(\cdot, 0)$ with f ,

$$f(z) = \sqrt{\frac{\pi}{K(0, 0)}} \int_0^z K(t, 0) dt,$$

(see [1, 8, 9, 13])

The numerical procedure for approximating f is based on the above properties and involves the following steps:

Step 1 Choose a complete set of functions $\{\eta_j\}_1^\infty$ for the space $L^2(\Omega)$.

Step 2 Orthonormalize the functions $\{\eta_j\}_1^n$ by means of the Gram-Schmidt process to obtain an orthonormal set $\{\eta_j^*\}_1^n$.

Step 3 Approximate the kernel function $K(\cdot, 0)$ by the Fourier sum

$$K_n(z, 0) = \sum_{j=1}^n \langle K(\cdot, 0), \eta_j^* \rangle \eta_j^*(z) = \sum_{j=1}^n \overline{\eta_j^*(0)} \eta_j^*(z)$$

Step 4 Approximate f by

$$f_n(z) = \sqrt{\frac{\pi}{K_n(0, 0)}} \int_0^z K_n(t, 0) dt.$$

The second step of the BKM involves the use of the Gram-Schmidt process which can be extremely unstable. For this reason we construct the Gramian matrix by using the Maple system, as this system provides integration routines so that the inner products involved can be computed without any loss of accuracy (cf. [11]).

2.2. Numerical Example.

In this section we present a simple example, just to illustrate the BKM. Consider the square

$$S := \{z = x + iy : |x| < 1, |y| < 1\}.$$

The usual choice of the basis set in **Step 1** is to take the polynomials $1, z, z^2, \dots$. In this example, because of the symmetry of S it suffices to consider the monomials $1, z^4, z^8, \dots$, the other inner products being zero, (see Gaier [8]). Denoting by n the number of monomials used, we have, for example, for $n = 2$,

$$\eta_1 = 1 \quad \text{and} \quad \eta_2 = z^4.$$

The corresponding ON functions are

$$\eta_1^* = \frac{1}{2} \quad \text{and} \quad \eta_2^* = \frac{1}{76}\sqrt{133} + \frac{15}{304}\sqrt{133}z^4,$$

the approximation K_2 to the Bergman kernel function is

$$K_2(z, 0) = \frac{83}{304} + \frac{105}{1216}z^4$$

and finally, the approximation f_2 to the conformal mapping function is

$$f_2(z) = \frac{1}{76}\sqrt{1577\pi}z + \frac{21}{25232}\sqrt{1577\pi}z^5.$$

Denote by ε_n the error estimate obtained by sampling the function $|1 - |f_n(z)||$ at a number of test points on ∂S . The following table contains the values of ε_n and the errors E_n corresponding to results presented in [11], for several values of n .

n	2	9	18	26	28
ε_n	$2.2E - 2$	$5.2E - 9$	$1.5E - 17$	$4.0E - 25$	$5.0E - 27$
E_n	–	$1.4E - 8$	$1.5E - 17$	$1.0E - 24$	–

TABLE 1. Errors estimates for the square

The results E_9 and E_{26} were obtained by Levin et al [12] and Papamichael et al [14], respectively, and are the best possible. The result E_{18} was obtained by Jank [11] by using the Maple system. At that time it was not possible to reach values of $n > 18$. Now it is clear that by using the Maple system and thus avoiding, whenever it is possible, the numeric Gram-Schmidt process, it is possible to obtain better results.

2.3. Numerical Difficulties.

If the domains under consideration are “difficult”, i.e. if there are singularities of the mapping function on or close to $\partial\Omega$, the convergence of the monomials is very slow. In such cases it is convenient to use the ideas of Levin, Papamichael and Sideridis [12] (see also ([14]) of including into the system of monomials $\{z^j\}_{j=0}^n$ functions that reflect these singularities. The package BKMPACK is a Fortran package, due to Warby [17] and is

based on the BKM with the so-called *augmented basis set* - BKM-AB. For example, for the L-shaped domain

$$\mathcal{L} := \{z = x + iy : -1 < x < 3, |y| < 1\} \cup \{z = x + iy : |x| < 1, y < 3\}$$

the use of BKM gives very poor approximations to the conformal map f , ($\varepsilon \approx 10^{-1}$). In fact, f has a serious branch point singularity at the re-entrant corner $z = 1 + i$ of \mathcal{L} .

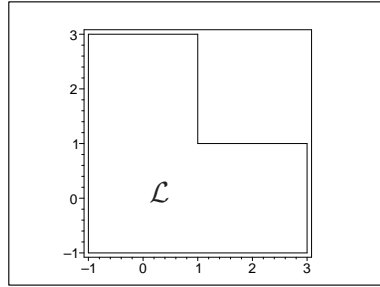


FIGURE 1. A “difficult” domain

The application of BKM-AB (with appropriated singular functions) can give more accurate approximations. The numerical implementation of BKM-AB produces an error $\varepsilon \approx 10^{-8}$ (see [14] for the details about the choice of the basis set and the numerical results).

Another well-known difficulty in conformal mapping is the *crowding* phenomenon. Crowding is a form of ill-conditioning that causes trouble in almost all numerical methods for conformal mapping. It occurs whenever the domain is *long*, that is, the target region has areas that are relatively long and thin. A common answer to this difficulty is to use a domain decomposition (see [6, 7]). As an example illustrating this difficulty, consider the rectangles

$$\mathcal{R}_a := \{z = x + iy : |x| < a, |y| < 1\}.$$

Next table contains the numerical results obtained by considering $a = 1, 2, 4, 6$ and 8 .

a	1	2	4	6	8
ε	$8.4E - 12$	$2.8E - 8$	$1.8E - 5$	$1.7E - 4$	$1.1E - 3$

TABLE 2. The effects of crowding

Here ε denotes the error estimate corresponding to $n = 25$. We note that in the case of the rectangle it is sufficient to consider the monomials $1, z^2, z^4, \dots$. For comparison purposes we consider also these monomials for $a = 1$, instead of $1, z^4, z^8, \dots$, as in last section.

3. FROM \mathbb{C} TO \mathbb{H}

3.1. Basic Notions and Results.

Let $\{1, e_1, e_2, e_3\}$ be an orthonormal base of the Euclidean vector space \mathbb{R}^4 with a product according to the multiplication rules

$$e_1^2 = e_2^2 = e_3^2 = -1, \quad e_1e_2 = -e_2e_1 = e_3.$$

This non-commutative product generates the algebra of real quaternions \mathbb{H} . The real vector space \mathbb{R}^4 will be embedded in \mathbb{H} by identifying the element

$$x = (x_0, x_1, x_2, x_3) \in \mathbb{R}^4$$

with the element

$$q = x_0 + e_1x_1 + e_2x_2 + e_3x_3 \in \mathbb{H}.$$

The conjugate of q is

$$\bar{q} = x_0 - e_1x_1 - e_2x_2 - e_3x_3.$$

Instead of the real and the imaginary parts we will distinguish between the scalar part of q

$$\text{Sc } q := x_0 = \frac{1}{2}(q + \bar{q})$$

and the vector part of q

$$\text{Vec } q := e_1x_1 + e_2x_2 + e_3x_3 = \frac{1}{2}(q - \bar{q}).$$

The norm $|q|$ of q is defined by

$$|q|^2 = q\bar{q} = \bar{q}q = x_0^2 + x_1^2 + x_2^2 + x_3^2$$

and it immediately follows that each non-zero $q \in \mathbb{H}$ has an inverse given by

$$q^{-1} = \frac{\bar{q}}{|q|^2}.$$

Introducing the hypercomplex variables

$$z_1 = -\frac{qe_1 + e_1q}{2} = x_1 - e_1x_0$$

and

$$z_2 = -\frac{qe_2 + e_2q}{2} = x_2 - e_2x_0,$$

we get

$$\mathbb{H}^2 = \{(z_1, z_2) : z_1 = x_1 - e_1x_0, z_2 = x_2 - e_2x_0\} \cong \mathbb{R}^3 \cong \mathcal{A} := \text{span}_{\mathbb{R}}\{1, e_1, e_2\}.$$

Now, let Ω be a domain in \mathbb{R}^3 and consider the \mathbb{H} -valued functions defined in Ω :

$$f : \mathbb{R}^3 \rightarrow \mathbb{R}^4 \cong \mathbb{H}$$

$$f(x) = f_0(x) + e_1f_1(x) + e_2f_2(x) + e_3f_3(x),$$

where $x = (x_0, x_1, x_2) \in \mathbb{R}^3$ and f_k are real valued in Ω functions. On the set $C^1(\Omega, \mathbb{H})$

define the quaternionic Cauchy-Riemann operator

$$D = \frac{\partial}{\partial x_0} + e_1 \frac{\partial}{\partial x_1} + e_2 \frac{\partial}{\partial x_2}$$

and its conjugate

$$\bar{D} = \frac{\partial}{\partial x_0} - e_1 \frac{\partial}{\partial x_1} - e_2 \frac{\partial}{\partial x_2}.$$

Definition 1. A C^1 -function f is called *left-monogenic* (resp. *right-monogenic*) in a domain Ω if

$$Df = 0, \text{ in } \Omega \quad (\text{resp. } fD = 0 \text{ in } \Omega).$$

Definition 2. If $\vec{z} = (z_1, z_2)$ then the “symmetric power ν ” of \vec{z} is defined as

$$\vec{z}^\nu := z_1^{\nu_1} \times z_2^{\nu_2} = \frac{\nu!}{|\nu|!} \sum_{\Pi(i_1, \dots, i_{|\nu|})} z_{i_1} \cdots z_{i_{|\nu|}},$$

where $\nu = (\nu_1, \nu_2)$ is a multi-index, $|\nu| = \nu_1 + \nu_2$, $\nu! = \nu_1! \nu_2!$ and the sum is taken over all permutations of $(i_1, \dots, i_{|\nu|})$.

Result 1. Let $\vec{z} = (z_1, z_2)$ and $\nu = (\nu_1, \nu_2)$. The permutational product $z_1^{\nu_1} \times z_2^{\nu_2}$ satisfies the recursion formula

$$z_1^{\nu_1} \times z_2^{\nu_2} = \frac{1}{\nu_1 + \nu_2} \{ \nu_1 (z_1^{\nu_1-1} \times z_2^{\nu_2}) z_1 + \nu_2 (z_1^{\nu_1} \times z_2^{\nu_2-1}) z_2 \}.$$

Result 2. Let $H_\nu^k(\vec{z}) := z_1^{\nu_1} \times z_2^{\nu_2}$, with $|\nu| = k$.

1. $H_\nu^k(\vec{z})$, are homogeneous polynomials of degree k .
2. $H_\nu^k(\vec{z})$, are monogenic functions.
3. $\{H_\nu^k(\vec{z})\} \cup \{1\}$ are a linearly independent system, for each $k \in \mathbb{N}$.

(These polynomials are also called *Fueter-polynomials*).

3.2. The Bergman Kernel Method.

The construction of reproducing kernel functions is not restricted to real dimension 2. Nowadays, reproducing kernels are a well known tool in the theory of functions of one or several complex variables and also in Clifford Analysis (for a review see [3, 10]). For more practical applications it is necessary to know the reproducing kernel explicitly. Results concerning the construction of Bergman kernel functions in closed form for special domains (the ball, the half-plane, strip domains, rectangular domains, etc) can be found in [3, 4, 5, 15, 16]. In this paper we construct the Bergman kernel function numerically and propose an analogous BKM for 3 dimensional cases.

Let Ω be a bounded simply-connected domain in \mathbb{R}^3 and denote by $L_r^2(\Omega, \mathbb{H})$ the right-Hilbert space of all square integrable \mathbb{H} -valued functions, endowed with the inner product,

$$(1) \quad \langle f(x), g(x) \rangle = \int_{\Omega} \overline{f(x)} g(x) dV.$$

The right linear set $L_r^2(\Omega, \mathbb{H}) \cap \ker D$ is a subspace in $L_r^2(\Omega, \mathbb{H})$ and has also a unique reproducing kernel $K(x, \zeta)$, i.e

$$\langle K(\cdot, \zeta), f \rangle = f(\zeta), \quad \forall f \in L_r^2(\Omega, \mathbb{H}) \cap \ker D.$$

and if we now take an orthonormal complete system of functions $\{\eta_j^*\}$ then it can be proved a Fourier series expansion for all functions $f \in L_r^2(\Omega, \mathbb{H}) \cap \ker D$

$$f(x) = \sum_{j=1}^{\infty} \eta_j^*(x) \langle \eta_j^*, f \rangle$$

and therefore

$$K(x, \zeta) = \sum_{j=1}^{\infty} \eta_j^*(x) \langle \eta_j^*, K(x, \zeta) \rangle = \sum_{j=1}^{\infty} \eta_j^*(x) \overline{\eta_j^*(\zeta)}.$$

This result suggests a numerical procedure to construct approximations to K similar to the complex case. More precisely, and assuming w.l.o.g. that $0 \in \Omega$, we rewrite **Steps 1-3** of BKM as follows:

Step 1 Choose a complete set of functions $\{\eta_j\}_1^\infty$ for the space $L_r^2(\Omega, \mathbb{H}) \cap \ker D$.

It is well known that the monogenic Fueter polynomials introduced in Section 3.1, H_ν^k , $|\nu| = k$; $k = 0, 1, \dots$, are a complete set of functions and are therefore the natural choice in this step.

Step 2 Orthonormalize the functions $\{\eta_j\}_1^n$ by means of the Gram-Schmidt process to obtain an orthonormal set $\{\eta_j^*\}_1^n$.

The use of Fueter polynomials up to degree N corresponds to a total of

$$n := \frac{(N+1)(N+2)}{2}$$

functions. More precisely, the n homogeneous polynomials of degree $\leq N$ are

$$\eta_j := H_{k-i,i}^k; \quad k = 0, \dots, N; \quad i = 0, \dots, k; \quad j = \frac{k(k+1)}{2} + i + 1.$$

Step 3 Approximate the kernel function $K(\cdot, 0)$ by the Fourier sum

$$K_N(x, 0) = \sum_{j=1}^n \eta_j^*(x) \overline{\eta_j^*(0)}; \quad N = 0, 1, \dots$$

All these results underline that the Clifford analysis and one complex variable analysis are closely connected. Thus, if we go further and introduce

Step 4 Compute

$$f_N(x) = C_N \int_0^x K_N(t, 0) dt; \quad N = 0, 1, \dots,$$

where C_N denotes some constant (depending on $K_N(0, 0)$), shall we get a “mapping” function from the domain Ω onto a sphere?

Before attempting to answer this question, we should make some remarks.

Remark 1. We don't expect f to be conformal as it is well known that in \mathbb{R}^3 the set of conformal mappings is restricted to the set of Möbius transformations as firstly shown by J. Liouville in 1850.

Remark 2. The polynomials η_j are in $\Omega \subset \mathbb{R}^3 \cong \mathcal{A} := \text{span}_{\mathbb{R}}\{1, e_1, e_2\}$, but the corresponding ON polynomials η_j^* are, in general, in $\mathbb{H} \cong \mathbb{R}^4$. This means that the kernel function K and the mapping function f are, in fact, functions from Ω in \mathbb{R}^4 .

Remark 3. From the geometric and practical point of view, we would like f to map domains $\Omega \subset \mathbb{R}^3$ to a sphere (for the moment, not necessarily the unit sphere).

Next two results are the starting point for the numerical BKM we propose.

Result 3. *If a function f of the form*

$$f = f(x) = f_0(x) + f_1(x)e_1 + f_2(x)e_2,$$

is left-monogenic then f is also right-monogenic.

Proof. Let $x = (x_0, x_1, x_2)$ and denote by ∂_k de partial derivatives $\frac{\partial}{\partial x_k}$, $k = 0, 1, 2$. If f is left-monogenic then

$$(\partial_0 + e_1\partial_1 + e_2\partial_2)(f_0 + f_1e_1 + f_2e_2) = 0,$$

and after some simple calculations, we get

$$\begin{cases} \partial_0 f_0 - \partial_1 f_1 - \partial_2 f_2 = 0 \\ \partial_1 f_0 + \partial_0 f_1 = 0 \\ \partial_2 f_0 + \partial_0 f_2 = 0 \\ \partial_1 f_2 - \partial_2 f_1 = 0 \end{cases}$$

and these conditions imply that f is right-monogenic, i.e.

$$(f_0 + f_1e_1 + f_2e_2)(\partial_0 + e_1\partial_1 + e_2\partial_2) = 0. \quad \square$$

Result 4. *Let $f : \Omega \subset \mathbb{H}^2 \rightarrow \mathbb{H} \cong \mathbb{R}^4$ be a function of the form*

$$f = f(x) = f_0(x) + f_1(x)e_1 + f_2(x)e_2 + f_3(x)e_3,$$

monogenic from both sides and such that

$$\exists a \in \Omega : f(a) = 0.$$

Then,

$$f_3 = 0, \quad \text{i.e.} \quad f : \mathbb{H}^2 \rightarrow \mathcal{A} \cong \mathbb{R}^3.$$

Proof. Let $f : \Omega \rightarrow \mathbb{H}$ be a function of the form

$$f = f(x) = f_0(x) + f_1(x)e_1 + f_2(x)e_2 + f_3(x)e_3.$$

If $D_L f = f D_R = 0$, then

$$\begin{cases} \partial_0 f_0 - \partial_1 f_1 - \partial_2 f_2 = 0 \\ \partial_1 f_0 + \partial_0 f_1 + \partial_2 f_3 = 0 \\ \partial_2 f_0 + \partial_0 f_2 - \partial_1 f_3 = 0 \\ \partial_1 f_2 - \partial_2 f_1 + \partial_0 f_3 = 0 \\ \partial_1 f_0 + \partial_0 f_1 - \partial_2 f_3 = 0 \\ \partial_2 f_0 + \partial_0 f_2 + \partial_1 f_3 = 0 \\ \partial_1 f_2 - \partial_2 f_1 - \partial_0 f_3 = 0 \end{cases}$$

This means that

$$\partial_0 f_3 = \partial_1 f_3 = \partial_2 f_3 = 0$$

and thus $f_3(x_0, x_1, x_2) = C$, where C is some constant. Therefore, f is a function of the form

$$f = f_0(x_0, x_1, x_2) + f_1(x_0, x_1, x_2)e_1 + f_2(x_0, x_1, x_2)e_2 + Ce_3.$$

Applying now the fact that $f(a) = 0$, for some $a \in \Omega$, we conclude that $C = f_3(a) = 0$ and the result is proved. \square

We don't expect f to be monogenic from both sides. We recall that Möbius transformations are the only conformal mappings in \mathbb{R}^{m+1} , ($m \geq 2$), but quaternionic Möbius transformations themselves are neither left nor right monogenic. However, Results 3 and 4 give the motivation for the numerical procedure we propose for computing f in Step 4 of BKM.

Step 4.1 Approximate the mapping function $g : \Omega \rightarrow \mathbb{H}$ by

$$(2) \quad g_N(x) = \int_0^x K_N(t, 0) dt; \quad N = 1, 2, \dots$$

Step 4.2 Approximate the mapping function f by “cutting” the “ e_3 -part” in (2), i.e. if g_N is of the form

$$(3) \quad g_N(x) = g_N^{\{0\}}(x) + g_N^{\{1\}}(x)e_1 + g_N^{\{2\}}(x)e_2 + g_N^{\{3\}}(x)e_3,$$

then construct the function f_N from Ω into $\mathcal{A} \cong \mathbb{R}^3$ by means of

$$(4) \quad f_N(x) = g_N^{\{0\}}(x) + g_N^{\{1\}}(x)e_1 + g_N^{\{2\}}(x)e_2.$$

3.3. Numerical Examples.

We illustrate this method by presenting some examples. All the numerical results presented in this work were obtained by using a specially developed Maple software package - `confMapPackage`, [2].

Example 1. Consider the cube

$$E_1 := \{(x_0, x_1, x_2) \in \mathbb{R}^3 : |x_0| < 1, |x_1| < 1, |x_2| < 1\},$$

and denote, as usual, by z_1 and z_2 the homogeneous polynomials $z_1 = x_1 - x_0e_1$ and $z_2 = x_2 - x_0e_2$. For example, for $N = 2$, the BKM details are as follows:

Step 1 The 6 homogeneous polynomials of degree ≤ 2 are:

$$\eta_1 := H_{(0,0)}^0(z_1, z_2) = 1,$$

$$\eta_2 := H_{(1,0)}^1(z_1, z_2) = x_1 - x_0 e_1,$$

$$\eta_3 := H_{(0,1)}^1(z_1, z_2) = x_2 - x_0 e_2,$$

$$\eta_4 := H_{(2,0)}^2(z_1, z_2) = x_1^2 - x_0^2 - 2x_0 x_1 e_1,$$

$$\eta_5 := H_{(1,1)}^2(z_1, z_2) = x_1 x_2 - x_0 x_2 e_1 - 2x_0 x_1 e_2,$$

$$\eta_6 := H_{(0,2)}^2(z_1, z_2) = x_2^2 - x_0^2 - 2x_0 x_2 e_2.$$

Step 2 The corresponding orthonormal polynomials are:

$$\eta_1^* = \frac{1}{4}\sqrt{2},$$

$$\eta_2^* = \frac{1}{4}\sqrt{3}(x_1 - x_0 e_1),$$

$$\eta_3^* = \frac{1}{4}\sqrt{3}(2x_2 - x_0 e_2 + x_1 e_3),$$

$$\eta_4^* = \frac{3}{56}\sqrt{70}(x_1^2 - x_0^2 - 2x_1 x_0 e_1),$$

$$\eta_5^* = \frac{3}{224}\sqrt{14}(14x_1 x_2 - 14x_2 x_0 e_1 - 4x_1 x_0 e_2 + (5x_1^2 - 5x_0^2)e_3),$$

$$\eta_6^* = \frac{3}{32}\sqrt{10}(-x_1^2 - x_0^2 + 2x_2^2 - 2x_2 x_0 e_2 + 2x_1 x_2 e_3).$$

Step 3 The approximation K_2 to the Bergman kernel function is

$$K_2(x, 0) = \frac{1}{8}, \quad x \in E_1.$$

Step 4 The approximation f_2 to the mapping function is

$$f_2(x) = \frac{1}{8}x, \quad x \in E_1.$$

Next figures correspond to the plots obtained with BKM for several values of N .

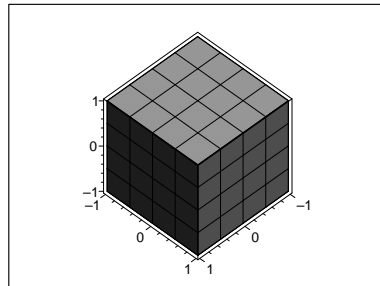


FIGURE 2. The original cube

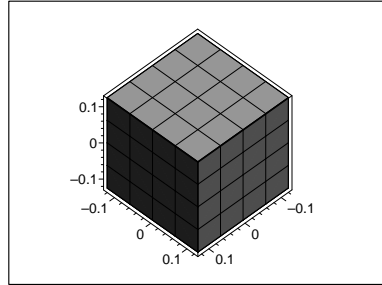


FIGURE 3. $N = 2$

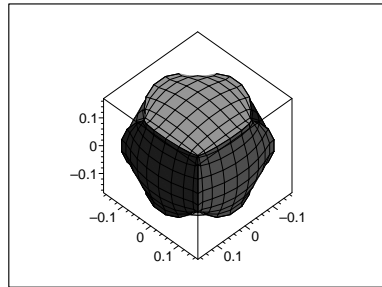


FIGURE 4. $N = 4$

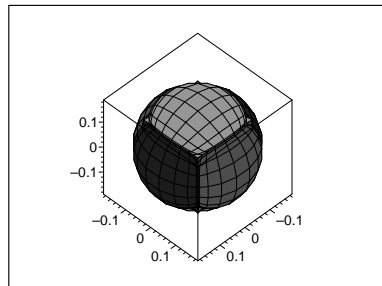


FIGURE 5. $N = 8$

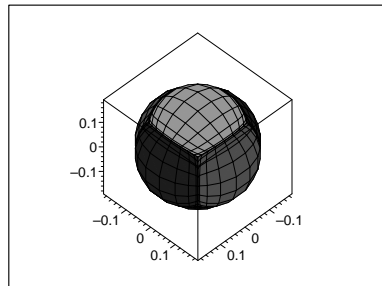


FIGURE 6. $N = 12$

The first obvious remark is that the image of the cube considered in Example 1 seems, in fact, to be a sphere, but not unitary. Moreover, numerical experiments show that the

constant factor

$$C_N := \sqrt{\frac{\pi}{K_N(0,0)}}$$

used in the complex case is not adequate. For the moment it is not completely clear what should be the choice of C_N .

The analysis of the “ e_3 -part” in (3), i.e. $g_N^{\{3\}}(x)$ shows some evidence that as N grows this function gets smaller. However we did not go further than $N = 14$, as our program becomes very time consuming. Figure 7 corresponds to the plot of $g_{14}^{\{3\}}(x)$, where $x \in \{(x_0, x_1, x_2) \in \mathbb{R}^3 : x_0 = 1, |x_1| < 1, |x_2| < 1\}$.

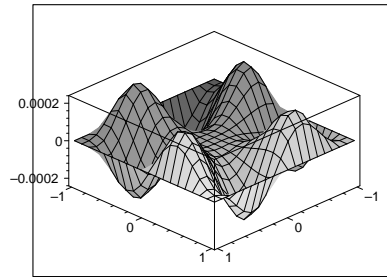


FIGURE 7. The function $g_{14}^{\{3\}}(x)$

Example 2. For the parallelepiped

$$E_2 := \{(x_0, x_1, x_2) \in \mathbb{R}^3 : |x_0| < 2, |x_1| < 1, |x_2| < 1\},$$

the BKM results are as follows:

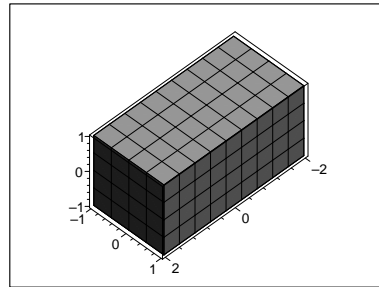


FIGURE 8. The original parallelepiped

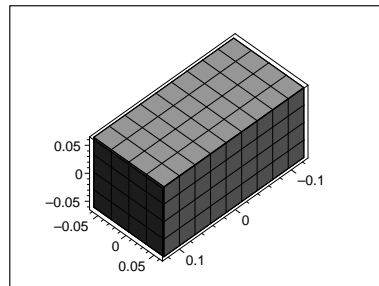


FIGURE 9. $N = 1$

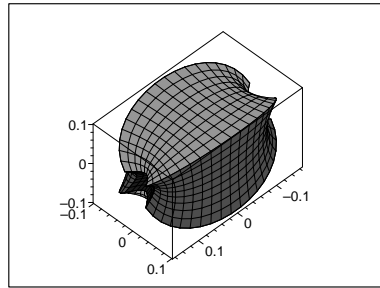


FIGURE 10. $N = 2$

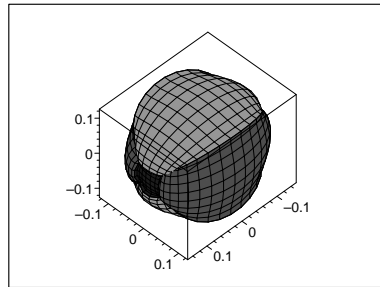


FIGURE 11. $N = 4$

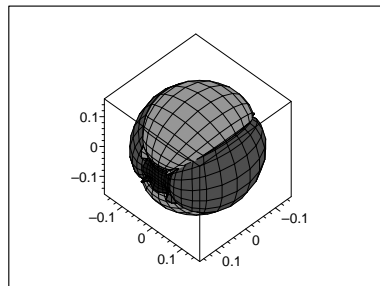


FIGURE 12. $N = 8$

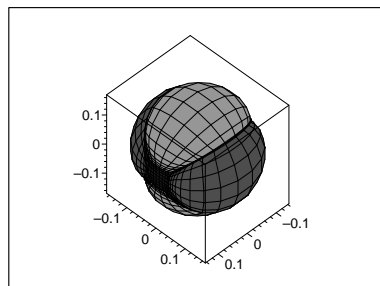
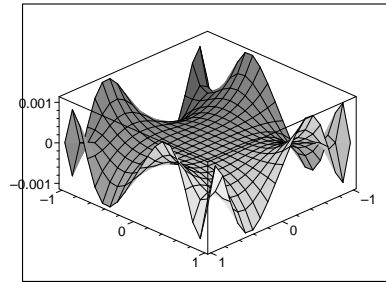


FIGURE 13. $N = 12$

Next figure corresponds to the plot of the function $g_{12}^{\{3\}}(x)$, for $x \in \{(x_0, x_1, x_2) \in \mathbb{R}^3 : x_0 = 2, |x_1| < 1, |x_2| < 1\}$.

FIGURE 14. The function $g_{12}^{\{3\}}(x)$

We end this section by presenting a last example of an L-shaped domain. Even for this “difficult” domain, the BKM results are very encouraging.

Example 3. Consider the L-shaped domain presented in Figure 15. The BKM results are as follows:

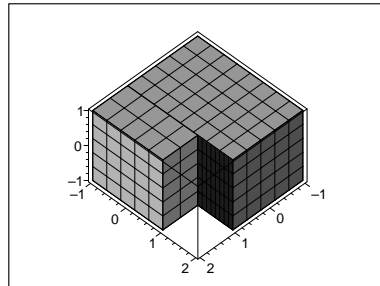
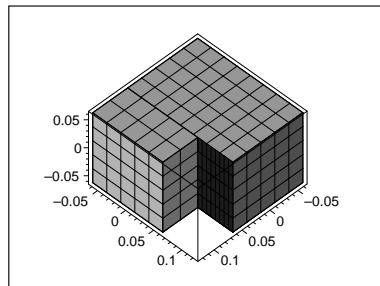
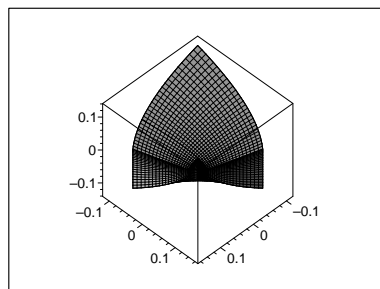


FIGURE 15. An L-shaped domain

FIGURE 16. $N = 0$ FIGURE 17. $N = 1$

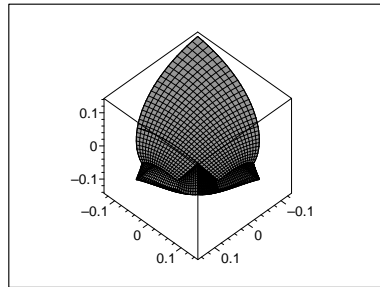


FIGURE 18. $N = 2$

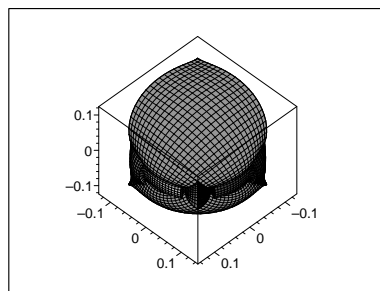


FIGURE 19. $N = 4$

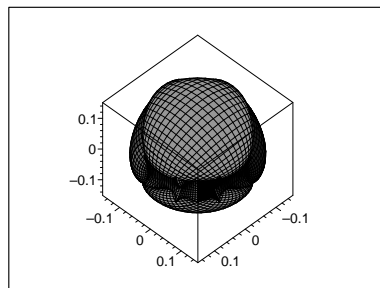


FIGURE 20. $N = 6$

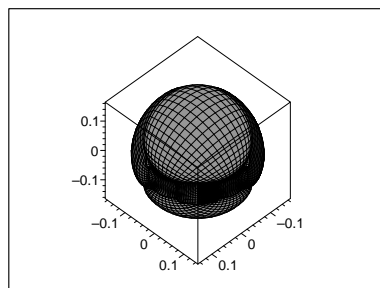


FIGURE 21. $N = 8$

4. CONCLUSIONS

Although we don't have for the moment a theoretical justification for the remarkable results achieved by the BKM propose (even for small values of N), we are convinced that this BKM-approach for 3 dimensional cases works and it is useful to continue the investigation in this direction. We expect to get theoretical results and to be able to improved this method by extending the complex idea of domain decomposition to higher dimensions.

REFERENCES

1. S. Bergman, *The kernel function and conformal mapping*, 2nd ed., Math. Surveys, vol. 5, Providence, R. I.: Americ. Math. Soc., 1970.
2. S. Bock, *Ansätze zur Approximation einer Klasse von Abbildungen ausgewählter dreidimensionaler Strukturen der Kontinuumsmechanik auf die Kugel*, Bauhaus-Universität Weimar, 2002.
3. F. Brackx, R. Delanghe, and F. Sommen, *Clifford analysis*, 76, Pitman, Boston-London-Melbourne, 1982.
4. D. Constales and R. S. Kraussnar, *Bergman kernels for rectangular and multiperiodic functions in Clifford analysis*, Math. Methods Appl. Sci. **25** (2002), no. 16-18, 1509–1526.
5. ———, *Szego and polynomogenic Bergman kernels for half-space and strip domains, and single-periodic functions in Clifford analysis*, Complex Variables Theory Appl. **47** (2002), no. 4, 349–360.
6. Tobin A. Driscoll and Lloyd N. Trefethen, *Schwarz-Christoffel mapping*, Cambridge Monographs on Applied and Computational Mathematics, 2002.
7. M. I. Falcão, N. Papamichael, and Stylianopoulos N. S., *Approximating the conformal maps of elongated quadrilaterals by domain decomposition*, Constructive Approximation **17** (2001), 589–617.
8. D. Gaier, *Konstruktive Methoden der konformen Abbildung*, Springer-Verlag, Berlin, 1964.
9. ———, *Lectures on complex approximation*, Birkhauser, Boston, 1987.
10. K. Gürlebeck and W. Sprössig, *Quaternionic and Clifford calculus for physicists and engineers*, John Wiley & Sons, 1997.
11. G. Jank and L. H. Tack, *Conformal mapping using Bergman's method and the MAPLE system*, ACM SIGSAM Bulletin **25** (1991), no. 2, 18–23.
12. D. Levin, N. Papamichael, and A. Sideridis, *The Bergman kernel method for numerical conformal mapping of simply connected domains*, J. Inst. Maths Applics. **22** (1978), 171–187.
13. Z. Nehari, *Conformal mapping*, McGraw-Hill, New York, 1952.
14. N. Papamichael and M. K. Warby, *Stability and convergence properties of Bergman kernel methods for numerical conformal mapping*, Numer. Math. **48** (1986), 639–669.
15. M.V. Shapiro and N.L. Vasilevski, *On the Bergman kernel function in hyperholomorphic analysis*, Acta Appl. Math. **46** (1997), 1–27.
16. N. L. Vasilevski, *On quaternionic Bergman and Poly-Bergman spaces*, Complex Variables Theory Appl. **41** (2000), 111–132.
17. M. K. Warby, *BKMPACK User's guide*, Tech. report, Dept of Maths and Stats, Brunel University, 1990.

S. BOCK
 Bauhaus-Universität Weimar
 D-99421 Weimar
 Germany
 bastian.bock@web.de

M. I. FALCÃO
 Centro Matemática
 Universidade do Minho
 4470 Braga
 Portugal
 mif@math.uminho.pt

K. GÜRLEBECK
 Bauhaus-Universität Weimar
 Institut Mathematik/Physik
 D-99421 Weimar
 Germany
 guerlebe@fossi.uni-weimar.de

H. MALONEK
 Dep. Matemática
 Universidade de Aveiro
 3810 Aveiro
 Portugal
 hrmalon@mat.ua.pt